An Optimal Decoding Algorithm for Molecular Communications Systems with Noise, Memory, and Pulse Width

Xiayang Wang[a], Yi Lu[a], Matthew D. Higgins[b,*], Mark S. Leeson[a]

[a] *School of Engineering, University of Warwick, Coventry, CV4 7AL, UK*
[b] *WMG, University of Warwick, Coventry, CV4 7AL, UK*

Abstract

Molecular Communications (MC) is a promising paradigm to achieve message exchange between nano-machines. Due to the specific characteristics of MC systems, the channel noise and memory significantly influence the MC system performance. Aiming to mitigate the impact of these two factors, an adaptive decoding algorithm is proposed by optimising the symbol determination threshold. In this paper, this novel decoding scheme is deployed onto a concentration-based MC system with the transmitter emission process considered. To evaluate the performance, an information theoretical approach is developed to derive the Bit Error Rate (BER) and the channel capacity. Simulations are also carried out to verify the accuracy of these formulations, to compare the performance difference against other decoding schemes, and to illustrate the performance deviation caused by different designing of relevant parameters. Furthermore, the performance of MC systems with the distance unknown is also analysed. Comparisons between distance-pre-known and distance-unknown systems are provided.

Keywords: Molecular Communications, Molecule Concentration, Decoding algorithm, Bit Error Rate, Capacity

1. Introduction

Molecular communications (MC) is an increasingly attractive idea, aiming to enable the networking of nano-machines. Molecules, encoded by the transmitter nano-machine (TN), propagate to the receiver nano-machine (RN) to accomplish the exchange of information. Such information can be expressed by either the number of certain molecules or the molecular concentration. In the first case, in [1, 2, 3, 4], researchers focused on the movement of individual molecules. There exists a certain probability for diffusing molecules to be captured by the RN, and the capture probability is utilised to describe the propagation mechanism. The RN is an active absorber, which can catch and remove the received molecules from the environment. By counting the number of captured molecules, the RN determines the information symbols. In the second case shown in [5, 6, 7, 8], attention has been paid to the molecular concentration. After being released from the TN, molecules will form a certain concentration distribution in the environment. The RN is assumed as a passive observer, which can sense the surrounding concentration to decode the message symbols without affecting the molecular distribution. No matter which way is chosen to express the information, the system performance is significantly impacted by the channel noise and memory. In order to alleviate the influence of these two factors, the decoding threshold of the RN should be optimised by considering previously transmitted symbols. Thus, an adaptive algorithm will be of great benefit to enhance the MC system performance by reducing the Bit Error Rate (BER) and improving the channel capacity.

By utilising amplitude modulation schemes, the decoding strategy of the RN is to compare the received molecular signal to a pre-designed threshold to determine whether '1' or '0' was transmitted. According to the adaptivity of the threshold, research analysing the MC system performance can be sorted into two classifications. In the first category, the threshold stays constant throughout the communication process. The MC system property with a fixed threshold was characterised in [1], and expanded in [2, 9] by taking the channel memory into consideration. Additionally, in [5, 10, 11, 12, 13, 14, 15], research that focused on modulation schemes and/or noise modelling, also provided theoretical approaches to evaluate the performance of MC systems with fixed thresholds. In these studies, messages were conveyed by the number of absorbed molecules, and the TN emission process was neglected by assuming that molecules were released simultaneously. As to the work considering the emission procedure [6, 16, 17], information was expressed by the molecular concentration. However, in these research, only simulations are carried out, rather than deriving mathematical expressions to study the MC system. In the second category, the decoding threshold varies depending on previously received symbols. In [4],

*Corresponding author

Email addresses: xiayang.wang@warwick.ac.uk (Xiayang Wang), yi.lu@warwick.ac.uk (Yi Lu), m.higgins@warwick.ac.uk (Matthew D. Higgins), mark.leeson@warwick.ac.uk (Mark S. Leeson)

the value of the threshold is designed to maximise a posteriori probability, but the system model should be refined by considering the emission effect. Other research such as [18, 19] has taken the emission process into account, and the threshold changes with regards to the previously decoded bits. However, the threshold should be further optimised to mitigate the influence of the channel memory and noise. Moreover, the impact of the channel memory still requires further investigation.

In this paper, the following contributions are presented. First, a new decoding algorithm is proposed by optimising the threshold with the aid of previously determined symbols. The optimal threshold is derived by a mathematical approach to minimise the BER of the MC system. Accordingly, expressions of the BER and capacity are obtained. Meanwhile, the impact of the TN emission over time is considered and the influence of the channel noise and memory are also clarified. Second, the impact of the ISI is further investigated even though it has been alleviated. For theoretical deviations, ISI length is treated as an arbitrary value to maximise the generality. For simulations it is set to a length of 20 such that results are of as a high precision as is reasonably practical. Third, this is the first paper to consider the distance estimation when analysing the MC channel. Before the communication is established, the RN measures the distance between the TN and itself, so that the RN can determine the sampling time and judging conditions correspondingly. The accuracy of the distance estimation will significantly affect the system performance.

The remainder of this paper is organised as follows. In Section 2 the communication model is introduced as well as the system structure. The new decoding algorithm and channel performance are presented in Section 3. Numerical results are provided in Section 4. Finally in Section 5, the paper is concluded.

2. The Concentration-Based Molecular Communications Model

As is illustrated in Fig. 1, the concentration-based MC system consists of two nano-machines, one of which, represented as Nano-machine A (NA), is viewed as the source nano-machine and the other, represented as Nano-machine B (NB), is viewed as the target nano-machine. In the first stage, before the communications between NA and NB are established, the NA emits a pulse of certain molecules (denoted as Molecule_1) to enable the NB to estimate the distance. Accordingly, the NB can adjust the sampling time and set the judging condition to determine whether '1' or '0' is transmitted. There exist several distance estimation schemes, such as those shown in [18, 20, 21]. In this paper, the scheme employing the peak concentration time to estimate the distance, proposed in [18], is selected for two reasons. Firstly, this scheme is implemented based on the same propagation model as the one utilised in this paper, which will be introduced later. Secondly, this scheme

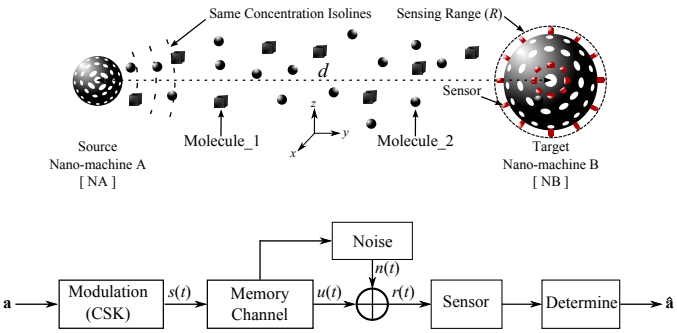

Figure 1: The structure and block diagram of the MC system.

provides a sufficiently accurate estimation, and is easy to implement due to its simplicity.

In the second stage of the communication process, the NA encodes information symbols into the concentration of another kind of molecule (denoted Molecule_2). Two kinds of molecules are utilised so that the distribution of 'estimation' molecules will not affect that of 'message' molecules. To transmit bit '1', the NA releases a certain amount of Molecule_2; to transmit bit '0', the NA stays quiet. The NB determines incoming messages by sensing the concentration around itself to a pre-designed threshold. In contrast to existing research, the design of the threshold is optimised by considering previous decoded symbols, which will be introduced later. Similar to the work in [6, 7, 8, 18, 22, 23], the concentration at the NB can be considered as the concentration at the centre of the sensing sphere.

The molecule concentration in a 3D environment is obtained by solving Fick's laws of diffusion, which can be regarded as the impulse response for the 3D diffusive channel [8, 22]:

$$h(d,t) = \frac{1}{(4\pi t D)^{3/2}} \exp\left(-\frac{d^2}{4tD}\right), \tag{1}$$

where d is the distance between the NA and NB (in µm), t is time (in µs), and D is the diffusion coefficient (in $\mu m^2\,\mu s^{-1}$).

The emission process, rather than being simplified as an impulse, is modelled as a rectangular pulse given by:

$$s(t) = \alpha \cdot \mathrm{rect}\left(\frac{t - T_e/2}{T_e}\right), 0 \le t \le T_p, \tag{2}$$

where α is the emission rate (in number/µs), T_e is the emission pulse duration (in µs) , T_p is the emission pulse period (in µs), and $T_e < T_p$. If m denotes the number of molecules released per pulse, it can be deduced that $m = \alpha \times T_e$. Therefore, the theoretical concentration at the NB, $u(d,t)$, formed by newly emitted molecules, can be obtained by the convolution operation $u(d,t) = s(t) *$

$h(d,t)$ [16], that is:

$$u(d,t) = \begin{cases} \frac{\alpha}{4\pi dD}\text{erfc}(\frac{d}{\sqrt{4tD}}), & t \le T_e \\ \frac{\alpha}{4\pi dD}\left[\text{erfc}(\frac{d}{\sqrt{4tD}}) - \text{erfc}(\frac{d}{\sqrt{4(t-T_e)D}})\right], & t > T_e \end{cases} \tag{3}$$

The NB is designed to sample the concentration at the time when theoretical concentration, $u(d,t)$, reaches the peak value. By deriving the equation $\frac{\partial u(d,t)}{\partial t} = 0$, the relationship between the distance and the sampling time T_0 can be obtained as [18]:

$$d^2 = \frac{6D}{T_e} \cdot (T_0 - T_e) \cdot T_0 \cdot \ln\left(\frac{T_0}{T_0 - T_e}\right). \tag{4}$$

Thus, by solving (4), the sampling time can be determined.

However, molecules will not vanish within one period T_p. The remaining molecules will have an influence on the concentration distribution of newly emitted molecules, which causes Inter-Symbol Interference (ISI). The existence time of newly emitted molecules is denoted as $(I+1) \times T_p$, after which the concentration referring to (3) is considered as negligible; I is called the ISI length. If this is infinite, the ISI brought in by the first pulse emission will affect all the following molecules signals; if it is finite, the channel is called a Memory Limited Channel (MLC) [24]. Thus, considering the ISI, the noiseless concentration at the NB can be regarded as the sum of the current signal concentration and previous ones, that is:

$$u^I(d,t) = \sum_{i=0}^{I} u(d, t = T_0 + i \times T_p) a_{k-i} = \sum_{i=0}^{I} u_i a_{k-i}, \tag{5}$$

where k represents the kth symbol from the beginning of transmission, the set $\{a_{k-i}, i = 0, 1, ..., I\}$ is the binary messages sequence, the element a_{k-i} represents the binary value of each symbol, and $\{u_i = u(d, T_0 + i \times T_p), i = 0, 1, 2, ..., I\}$. During the diffusion process, an additive signal-dependent noise, $n(t)$, will also affect the concentration at the NB. The noise, $n(t)$, is normally distributed with the expression given as [6, 8, 18, 19, 23]:

$$n(t) \sim \mathcal{N}(0, \sigma^2), \tag{6}$$

where $\sigma^2 = \frac{3}{4\pi R^3} u^I(t) = \frac{3}{4\pi R^3} \sum_{i=0}^{I} u_i a_{k-i}$. Consequently, referring to Fig. 1, the concentration at the NB can be derived as:

$$r(d, t = T_0) = u^I(d,t) + n(t = T_0) = \sum_{i=0}^{I} u_i a_{k-i} + n(t = T_0). \tag{7}$$

As defined in [6], the signal power and noise power of the MC system are respectively obtained by:

$$W_u = u_0^2, \tag{8}$$

$$W_n = E[n(t)^2], \tag{9}$$

where $E[\cdot]$ represents the expectation value. Given (6), the value of $E[n(t)^2]$ can be derived as:

$$\begin{aligned} E[n(t)^2] = E[\sigma^2] &= E\left[\frac{3u(t)}{4\pi R^3}\right] = \frac{3}{4\pi R^3} E[u(t)] \\ &= \frac{3}{4\pi R^3} E\left[\sum_{i=0}^{I} u_i a_{k-i}\right] = \frac{3p}{4\pi R^3} \sum_{i=0}^{I} u_i, \end{aligned} \tag{10}$$

where p is the probability of symbol '1' transmitted.

Given (8) to (10), the Signal-to-Noise-Ratio (SNR) at the NB for this MC system can be calculated as[6]:

$$\text{SNR} = \frac{W_u}{W_n} = \frac{u_0^2}{\frac{3p}{4\pi R^3} \sum_{i=0}^{I} u_i} = \frac{4\pi R^3 u_0^2}{3p \sum_{i=0}^{I} u_i}. \tag{11}$$

3. Channel Analysis

The NB is designed to determine the message bits by comparing the received concentration to a pre-designed threshold η. Thus, given $r(d, t = T_0)$ representing the sensed concentration, the judgement condition L can be expressed as:

$$L = r(d, t = T_0) - \eta. \tag{12}$$

The design of η has taken the influence of both previous symbols and the noise into consideration, which is a method to mitigate the influence of the channel memory and noise. The method for η optimisation will be introduced later in this paper. When $L \ge 0$, '1' is decided; otherwise, '0' is decided. Considering $r(d, t = T_0)$ in (7), the threshold η can be designed with an expression given as [25]:

$$\eta = \sum_{i=1}^{I} u_i \hat{a}_{k-i} + \tau \tag{13}$$

where $0 < \tau < u_0$, and the set $\{\hat{a}_{k-i}, i = 1, 2, ..., I\}$ is previously decoded bits within the ISI length I. If errors are assumed to occur independently, then previously decoded bits will not affect the decoding of the current symbol. Thus, in this case, it is assumed that $\hat{a}_{k-i} = a_{k-i}$ for $i = 1, 2, ..., I$. By substituting (7) and (13) into (12), L can be derived as:

$$L = n(t = T_0) + a_k u_0 - \tau. \tag{14}$$

3.1. Bit Error Rate analysis

Error occurs only in two scenarios; when '0' is transmitted but '1' is received (named as a_k=0 but $\hat{a}_k$=1), or when '1' is transmitted but '0' is received (named as a_k=1 but $\hat{a}_k$=0). Due to the existence of the ISI, different permutations of the values of $\{a_{k-i}, i = 1, 2, ..., I\}$ will result in different error patterns. Each error pattern will correspond to a certain permutation of values of $\{a_{k-i}, i = 1, 2, ..., I\}$. With the ISI length equal to I, there will be 2^I error patterns. In this work, 'j' denotes the error pattern index,

where $j = 1, 2, ..., 2^I$. For the error pattern 'j', the number of '1's within the previous symbols $\{a_{k-i}, i = 1, 2, ..., I\}$ is denoted as ϱ, and the number of '0's is $(I - \varrho)$.

(1) a_k=0, but $\hat{a}_k$=1:

With $a_k = 0$, to obtain the condition $L \geq 0$ in (14), it is required that:

$$n(t = T_0) \geq \tau. \tag{15}$$

Given (6), the probability for the error pattern 'j' with '0' transmitted can be derived by calculating the probability of $n(t = T_0) \geq \tau$, that is:

$$\begin{aligned} P_{e0j} &= p^{\varrho_j}(1-p)^{I-\varrho_j} \int_{\tau}^{\infty} \frac{1}{\sqrt{2\pi}} \frac{1}{\sigma_{0j}} \exp(-\frac{v^2}{2\sigma_{0j}^2}) dv \\ &= p^{\varrho_j}(1-p)^{I-\varrho_j} \left(1 - \Phi\Big(\frac{\tau}{\sigma_{0j}}\Big)\right) \\ &= p^{\varrho_j}(1-p)^{I-\varrho_j} \Phi\Big(\frac{-\tau}{\sigma_{0j}}\Big), \end{aligned} \tag{16}$$

where $\sigma_{0j} = \sqrt{\frac{3}{4\pi R^3} \sum_{i=1}^{I} a_{k-i} u_i}$.

(2) a_k=1, but $\hat{a}_k$=0:

With $a_k = 1$, to obtain the condition $L < 0$ in (14), it is required that:

$$n(t = T_0) < \tau - u_0. \tag{17}$$

Given (6), the probability for the error pattern 'j' with '1' transmitted can be obtained as:

$$\begin{aligned} P_{e1j} &= p^{\varrho_j}(1-p)^{I-\varrho_j} \int_{-\infty}^{\tau-u_0} \frac{1}{\sqrt{2\pi}} \frac{1}{\sigma_{1j}} \exp(-\frac{v^2}{2\sigma_{1j}^2}) dv \\ &= p^{\varrho_j}(1-p)^{I-\varrho_j} \left(1 - \Phi\Big(\frac{u_0 - \tau}{\sigma_{1j}}\Big)\right) \\ &= p^{\varrho_j}(1-p)^{I-\varrho_j} \Phi\Big(\frac{\tau - u_0}{\sigma_{1j}}\Big), \end{aligned} \tag{18}$$

where $\sigma_{1j} = \sqrt{\frac{3}{4\pi R^3}(\sum_{i=1}^{I} a_{k-i} u_i + u_0)}$.

(3) Bit Error Rate:

The BER can be derived as:

$$\begin{aligned} P_e &= (1-p)P_{e0} + pP_{e1} \\ &= (1-p)\sum_{j=1}^{2^I} P_{e0j} + p\sum_{j=1}^{2^I} P_{e1j}, \end{aligned} \tag{19}$$

where $P_{e0} = \sum_{j=1}^{2^I} P_{e0j}$, and $P_{e1} = \sum_{j=1}^{2^I} P_{e1j}$. Table 1 is an example showing the probabilities of each error pattern for $I = 2$.

(4) Optimise τ to minimise the error rate for each error pattern:

Aiming to achieve the minimum BER, it is required that the error rate of each pattern 'j' should be minimised by carefully selecting the value of τ in (16) and (18). Thus, for a certain error pattern 'j', $j = 1, 2, 3, ..., 2^I$, the sum of error rates for either '1' or '0' transmitted can be expressed as:

$$\begin{aligned} P_{ej} &= p \cdot P_{e1j} + (1-p)P_{e0j} \\ &= p^{\varrho_j}(1-p)^{I-\varrho_j} \left[p \cdot \Phi\Big(\frac{\tau - u_0}{\sigma_{1j}}\Big) + (1-p)\Phi\Big(\frac{-\tau}{\sigma_{0j}}\Big)\right]. \end{aligned} \tag{20}$$

Hence, the equation $\frac{\partial P_{ej}}{\partial \tau} = 0$ needs to be solved:

$$\begin{aligned} \frac{\partial P_{ej}}{\partial \tau} = p^{\varrho_j}(1-p)^{I-\varrho_j} \Bigg[& p \cdot (\frac{1}{\sigma_{1j}}) \frac{1}{\sqrt{2\pi}} \exp\Big(-\frac{(u_0-\tau)^2}{2\sigma_{1j}^2}\Big) - \\ & (1-p)(\frac{1}{\sigma_{0j}}) \frac{1}{\sqrt{2\pi}} \exp\Big(-\frac{(\tau)^2}{2\sigma_{0j}^2}\Big)\Bigg] = 0. \end{aligned} \tag{21}$$

Considering $0 < \tau < u_0$, by solving (21), the optimal value of τ, represented as τ_o, can be obtained as:

$$\tau_o = \frac{-\sigma_{0j}^2 u_0 + \sigma_{0j}\sigma_{1j}\sqrt{u_0^2 - 2(\sigma_{1j}^2 - \sigma_{0j}^2) \cdot \ln\left(\frac{p \cdot \sigma_{0j}}{(1-p)\sigma_{1j}}\right)}}{\sigma_{1j}^2 - \sigma_{0j}^2}. \tag{22}$$

By substituting (22) into (16), (18), and (19), the minimised BER can be derived. Particularly, if $\tau = \frac{u_0}{2}$, the threshold is the same as the one utilised in [18, 19].

3.2. Capacity analysis

The binary input vector of the system is denoted by $\mathbf{X} = \{X_1, X_2, ..., X_k\}$, and the corresponding binary output vector is denoted by $\mathbf{Y} = \{Y_1, Y_2, ..., Y_k\}$. Thus, the capacity for the memory channel can be calculated from [11]:

$$\text{Capacity} = \lim_{k\to\infty} \max_{p} \sum_{i=1}^{k} \frac{1}{k} \mathcal{I}(X_i; Y_i), \tag{23}$$

where $\mathcal{I}(X_i; Y_i)$ is the mutual information defined as [11]:

$$\begin{aligned} \mathcal{I}(X_i; Y_i) &= H(Y_i) - H(Y_i|X_i) \\ &= \mathcal{H}[(1-p)(1-P_{e0}) + pP_{e1}] \\ &\quad - p\mathcal{H}(1-P_{e1}) - (1-p)\mathcal{H}(1-P_{e0}), \end{aligned} \tag{24}$$

where $\mathcal{H}(\xi) = -\xi \log_2 \xi - (1-\xi)\log_2(1-\xi)$. If the channel is a memory unlimited channel with an infinite ISI length I, the capacity can be calculated by substituting (16), (18), (19) and (24) into (23).

For an MLC with finite ISI length I, after the ith symbol ($i > I + 1$), the newly emitted molecular signal will be affected by the same amount (equal to I) of previous signals. Referring to (16)-(19), it can be deduced that the average error probability stays constant after the ith symbol ($i > I + 1$). Thus, with p fixed and values of P_{e0} and P_{e1} being constant, it can be proven from (24) that:

$$\mathcal{I}(X_i; Y_i) = \mathcal{I}(X_{I+1}; Y_{I+1}), \forall i \in \{I+1, I+2, ..., k\}. \tag{25}$$

Table 1: Error patterns and the probabilities for ISI length $I = 2$.

Index	ISI		Variance		Probability of each error pattern	
j	a_{k-2}	a_{k-1}	σ_{0j}^2	σ_{1j}^2	P_{e0j} (a_k=0 but $\hat{a}_k$=1)	P_{e1j} (a_k=1 but $\hat{a}_k$=0)
1	0	0	0	$\frac{3u_0}{4\pi R^3}$	0	$(1-p)^2 \cdot \Phi(\frac{\tau-u_0}{\sigma_{11}})$
2	0	1	$\frac{3u_1}{4\pi R^3}$	$\frac{3(u_1+u_0)}{4\pi R^3}$	$p(1-p) \cdot \Phi(\frac{-\tau}{\sigma_{02}})$	$p(1-p) \cdot \Phi(\frac{\tau-u_0}{\sigma_{12}})$
3	1	0	$\frac{3u_2}{4\pi R^3}$	$\frac{3(u_2+u_0)}{4\pi R^3}$	$p(1-p) \cdot \Phi(\frac{-\tau}{\sigma_{03}})$	$p(1-p) \cdot \Phi(\frac{\tau-u_0}{\sigma_{13}})$
4	1	1	$\frac{3(u_1+u_2)}{4\pi R^3}$	$\sum_{i=0}^{2} \frac{3u_i}{4\pi R^3}$	$p^2 \cdot \Phi(\frac{-\tau}{\sigma_{04}})$	$p^2 \cdot \Phi(\frac{\tau-u_0}{\sigma_{14}})$

Thus, for the MLC, the capacity calculation can be simplified as:

$$\begin{aligned}
\text{Capacity} &= \lim_{k\to\infty} \max_p \Big\{ \sum_{i=1}^{k} \frac{1}{k} \mathcal{I}(X_i;Y_i) \Big\} \\
&= \lim_{k\to\infty} \max_p \left\{ \sum_{i=1}^{I} \frac{1}{k} \mathcal{I}(X_i;Y_i) + \sum_{j=I+1}^{k} \frac{1}{k} \mathcal{I}(X_j;Y_j) \right\} \\
&= \lim_{k\to\infty} \max_p \left\{ \sum_{i=1}^{I} \frac{1}{k} \mathcal{I}(X_i;Y_i) \right\} \\
&\qquad + \lim_{k\to\infty} \max_p \left\{ \frac{k-I}{k} \mathcal{I}(X_{I+1};Y_{I+1}) \right\} \\
&= 0 + \max_p \{\mathcal{I}(X_{I+1};Y_{I+1})\} \\
&= \max_p \{\mathcal{I}(X_{I+1};Y_{I+1})\}. \qquad (26)
\end{aligned}$$

By substituting (16), (18), (19) and (24) into (26), the capacity for MLC can be obtained.

3.3. Utilising the distance estimation scheme

If the distance is unknown, it is required that the distance estimation process should be implemented. The NA emits a pulse of molecules, and the NB keeps sensing the concentration around itself to find the peak time of the concentration, based on which, the distance between the NA and NB can be determined. Hence, the peak time can be considered as the sampling time for the NB, denoted as $\hat{T}_0$. Considering (4), the distance is determined, denoted as $\hat{d}$. Thus, during the communications stage, the sampled concentration $r(t)$ can be derived as:

$$\begin{aligned}
r(d, t=\hat{T}_0) &= \sum_{i=0}^{I} a_{k-i} u(d; t=\hat{T}_0 + iT_p) + n(t=\hat{T}_0) \\
&= \sum_{i=0}^{I} a_{k-i} u_i^d + n(t=\hat{T}_0), \qquad (27)
\end{aligned}$$

and the expression for η can be expressed as:

$$\begin{aligned}
\eta &= \sum_{i=1}^{I} \hat{a}_{k-i} u(\hat{d}, t=\hat{T}_0 + iT_p) + \tau' \\
&= \sum_{i=1}^{I} \hat{a}_{k-i} u_i^{\hat{d}} + \tau', \qquad (28)
\end{aligned}$$

Similarly, it is also assumed that $\hat{a}_{k-i} = a_{k-i}$ for $i = 1, 2, ..., I$. By substituting (27) and (28) into (12), L can be derived as:

$$\begin{aligned}
L &= \sum_{i=1}^{I} a_{k-i}(u_i^d - u_i^{\hat{d}}) + a_k u_0^d + n(t=\hat{T}_0) - \tau', \\
&= a_k u_0^d + n(t=T_0) - \tau' + \beta. \qquad (29)
\end{aligned}$$

where $\beta = \sum_{i=1}^{I} a_{k-i}(u_i^d - u_i^{\hat{d}})$ is substituted to make it easier to follow.

Similar to the derivation in Section 3.1, the probability for the error pattern j can be obtained as:

$$P_{e1j}^{\hat{d}} = p^{\varrho_j}(1-p)^{I-\varrho_j}\left(1 - \Phi\Big(\frac{u_0 - \tau' + \beta}{\sigma_{1j}^{\hat{d}}}\Big)\right), \qquad (30)$$

$$P_{e0j}^{\hat{d}} = p^{\varrho_j}(1-p)^{I-\varrho_j}\left(1 - \Phi\Big(\frac{\tau' - \beta}{\sigma_{0j}^{\hat{d}}}\Big)\right), \qquad (31)$$

where

$$\sigma_{1j}^{\hat{d}} = \sqrt{\frac{3}{4\pi R^3}(\sum_{i=1}^{I} a_{k-i} u_i^d + u_0^d)}, \qquad (32)$$

$$\sigma_{0j}^{\hat{d}} = \sqrt{\frac{3}{4\pi R^3}(\sum_{i=1}^{I} a_{k-i} u_i^d)}. \qquad (33)$$

Correspondingly, the optimal value of τ', represented as τ'_o, can be derived as:

$$\tau'_o = \frac{-(\sigma_{0j}^{\hat{d}})^2 u_0 + \sigma_{0j}^{\hat{d}}\sigma_{1j}^{\hat{d}}\sqrt{u_0^2 - 2\Big((\sigma_{1j}^{\hat{d}})^2 - (\sigma_{0j}^{\hat{d}})^2\Big) \cdot \ln\left(\frac{p \cdot \sigma_{0j}^{\hat{d}}}{(1-p)\sigma_{1j}^{\hat{d}}}\right)}}{(\sigma_{1j}^{\hat{d}})^2 - (\sigma_{0j}^{\hat{d}})^2} \qquad (34)$$

Thus, the BER for MC systems with the distance estimation scheme utilised can be computed as:

$$P_e^{\hat{d}} = (1-p)P_{e0}^{\hat{d}} + pP_{e1}^{\hat{d}}$$
$$= (1-p)\sum_{j=1}^{2^I} P_{e0j}^{\hat{d}} + p\sum_{j=1}^{2^I} P_{e1j}^{\hat{d}}, \quad (35)$$

4. Numerical Results

In this section, numerical results for both MATLAB simulations and theoretical derivations are presented. During the simulations, the NA emits molecules periodically. Such molecules spread out and form a concentration distribution in the environment. The NB samples the concentration around itself at time T_0 (or $\hat{T}_0$) in each period, based on which, the NB determines whether '1's or '0's are transmitted. The times of simulation trials are based on the theoretically derived results, and are designed to be sufficient to reach the required accuracy. For example, if the theoretical BER is 10^{-4}, then 10^8 successive bits are utilised to carry out the corresponding simulations. All results are presented with a common set of parameters assigned in Table 2. These values agree with the research in [2, 6, 7, 18, 19]. Further denotation is that the optimal threshold proposed in this paper is represented as 'OT', and the decoding algorithm proposed in [19] is represented as 'MSE'.

It should be noticed that when the ISI length I increases, not only the computation of the BER and capacity increases exponentially, but also simulations will become more complex to perform. Particularly, if I is infinite, it is impossible to obtain the required results. Thus, the channel considered herein is an MLC with a finite I. The value of I used in this paper has been greatly increased compared with all existing work, and we believe it is sufficiently large for the MC system analysis. If further results for larger I are required, readers could compute the BER and capacity based on (16) to (35).

4.1. The concentration affected by the emission duration

Fig. 2 shows the change in concentration around the NB with respect to time. It can be noticed that the emission duration T_e is influential to the concentration distribution. Firstly, the rising T_e will lead to the decrease in the peak concentration u_0. The increase of T_e means the NA emits molecules more slowly, and these molecules start to propagate to the infinite border immediately upon being released. By the time the NA finishes the emission, a certain number of molecules have diffused widely in the environment. Thus, the peak concentration around the NB would be correspondingly smaller.

Secondly, the rising T_e will result in the increasing concentration tails after one pulse period, namely $(u_i, i = 1, 2, ..., I)$. It has been explained that a smaller u_0 will be obtained by enlarging T_e. In other words, the concentration gradient is gentler, and therefore after the peak time,

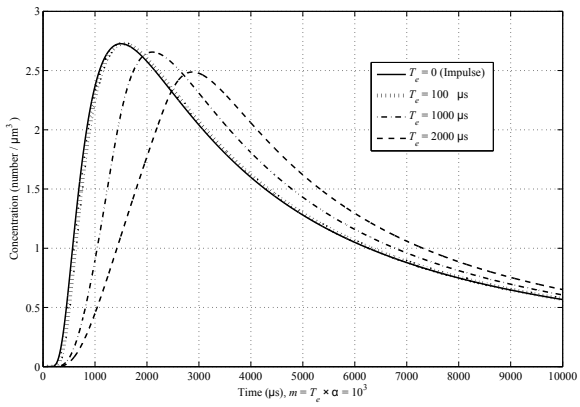

Figure 2: The change of concentration with time for different T_e at $d = 3\,\mu$m.

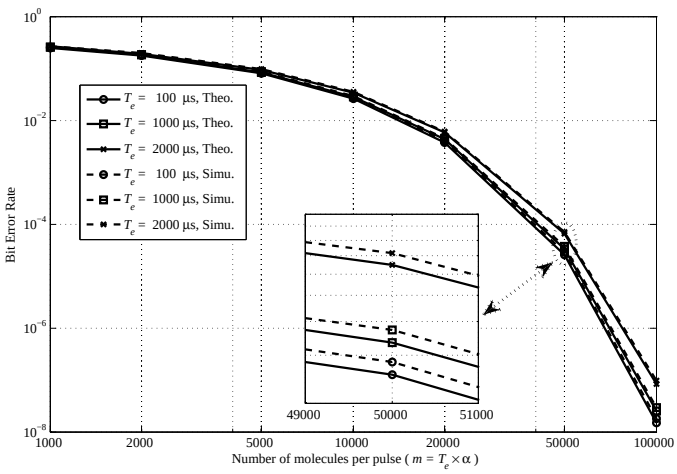

Figure 3: BER Vs. m for different T_e with $I = 20$ and $d = 3\,\mu$m.

molecules will diffuse to the infinite border in a lower rate, which means the attenuation of the concentration will be correspondingly slower. As a consequence, the concentration tails will be enlarged.

Referring to (11), either the decrease of the peak concentration (u_0) or the increase of the tail $(u_i, i = 1, 2, ..., I)$ will lead to a smaller SNR. Then, it can be deduced that the MC system with a large T_e will exhibit a worse performance, which agrees with the curves shown in Figs. 3 to 5.

4.2. Channel performance analysis for OT decoding algorithm

Results for the performance analysis are presented in Figs. 3 to 5. It can be seen that the BER and capacity are mainly influenced by three factors, namely, the number of molecules emitted per pulse (m), the emission duration (T_e), and the ISI length (I). According to (3)-(11), the change of these three parameters affects the SNR of the channel, which will have a corresponding impact on the channel performance in terms of the BER and capacity.

Table 2: Simulation parameters

1.	The radium of the NB	R	$0.5\,\mu\text{m}$
2.	The distance between NA and NB	d	$2 \sim 4\mu\text{m}$
3.	The diffusion coefficient	D	$10^{-3}\mu\text{m}^2\,\mu\text{s}^{-1}$
4.	The emission duration	T_e	$100 \sim 2000\mu\text{s}$
5.	The pulse period	T_p	$5000\,\mu\text{s}$
6.	The number of transmitted molecules	m	$10^3 \sim 10^5$

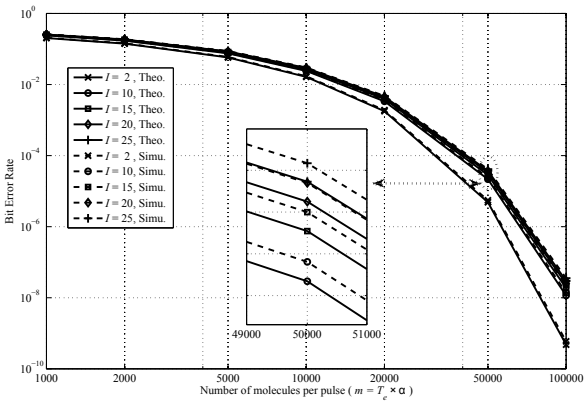

Figure 4: BER Vs. m for different I with $T_e = 1000\,\mu\text{s}$ and $d = 3\,\mu\text{m}$.

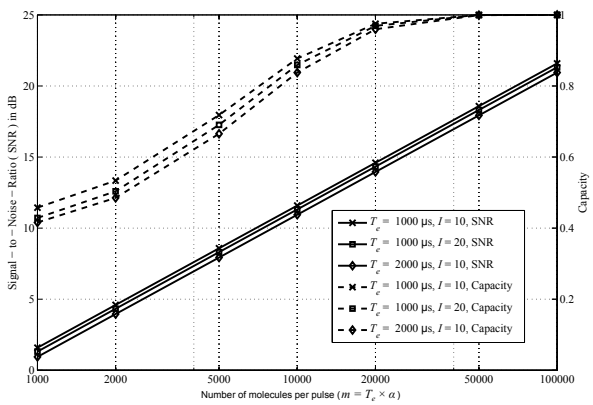

Figure 5: SNR and capacity Vs. m for different I and T_e with $d = 3\,\mu\text{m}$.

To be specific, in Figs. 3 to 5, increasing m will help the system to suffer less from errors and achieve a higher capacity. The reason is that with more molecules emitted per pulse, the system will have a stronger resistance against the noise and ISI. Referring to (3)-(11), amplifying m leads to a larger SNR, which guarantees a better performance.

The change in T_e will also affect the BER and capacity of the system. In Figs. 3 and 5, decreasing T_e leads to a smaller BER and higher capacity. As is explained in Section 4.1, the reduction of T_e brings about a larger SNR. Thus, if the NA emits molecules as fast as possible, the channel performance can be enhanced.

Another factor that influences the system is the ISI length. Even though the influence of the ISI has been mitigated by using the decoding method described by (12) to (14), it can be deduced from (6) that the remaining concentrations of previous bits will contribute to the noise effect. Consequently, the ISI will still affect the channel performance. If the ISI can be further alleviated, a smaller BER and higher capacity will be obtained. This shows agreement with the results in Figs. 4 and 5 that decreasing I also results in a larger SNR because molecules vanish more quickly so that less influence will be brought onto the upcoming signals. Moreover, as is also clearly shown here, there is no significant difference in performance between $I = 15, 20,$and 25. Thus, considering the fact that with I rising, the complexity of both the computation of BER and capacity and MATLAB simulations increases exponentially, $I = 20$ is sufficiently large for system performance analysis.

It should also be noticed that the simulated BER is slightly higher than the theoretical BER even if the deviation is almost negligible. The main reason of the difference herein is that the assumption that errors occur independently for theoretical derivation does not hold during simulations. In other words, when decoding the bit a_k, for theoretical derivation, it is assumed that $\hat{a}_{k-i} = a_{k-i}$ for $i = 1, 2, ..., I$; while for simulations, one wrongly decoded bit will affect the decoding of next several symbols. Errors therefore occur in succession, which is called *Error Propagation*. Additionally, during simulations, there is a chance that the concentration may rise to a high value and takes time to recover to a normal level, which also affects the decoding of next several symbols. This also causes the Error Propagation, leading to a higher BER for simulations.

An important but not intuitive feature shown throughout Figs. 3 to 5 is that no matter how parameters are selected, the performance almost remains the same if the system SNR remains constant. An example is shown in Fig. 6 where the BER for MC systems with different parameters is presented. As is illustrated there, although the assignment of parameters varies, the difference in the error probabilities of MC systems with the same SNR is so small that it can be neglected. Therefore, the SNR, defined in (11), can be considered as a reasonable metric to evaluate the diffusive concentration-based MC system performance.

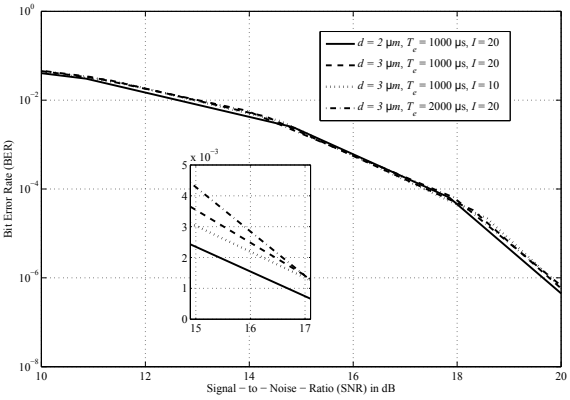

Figure 6: BER Vs. SNR for different parameter assignment.

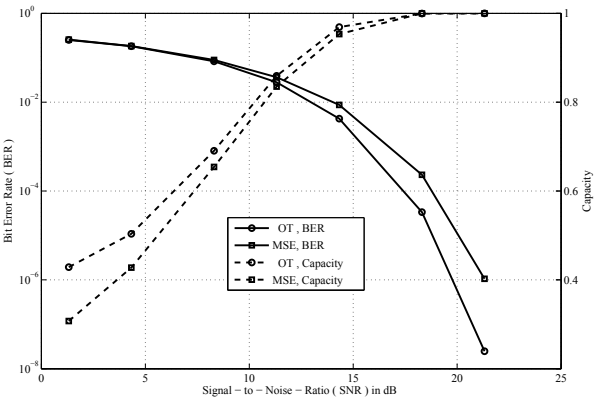

Figure 7: Performance comparisons between OT and MSE with $I = 20$, $T_e = 1000\,\mu\text{s}$, and $d = 3\,\mu\text{m}$.

4.3. Channel performance comparisons between OT and MSE decoding algorithms

In Fig. 7, the performance enhancement by using OT rather than MSE is presented. For MSE, the parameter τ of the threshold η is set to be $\tau = \frac{u_0}{2}$, while for OT, the value of τ is optimised according to different error patterns. By coordinating τ, the BER for each error pattern has been minimised. Consequently, the concentration-based MC system tends to enjoy a lower error rate and a better maximum reliable transmission rate. However, this performance improvement is brought in at the cost of a higher requirement on the complexity of the NB. As expressed in (22), the optimal value of τ keeps changing through the communications process, and requires the NB to determine the corresponding optimal τ_o within the time less than a pulse period T_p, which may exceed the capability of nano-machines. Hence, when choosing the decoding algorithms, not only should the system performance be taken into account, but also the complexity of nano-machines needs to be considered.

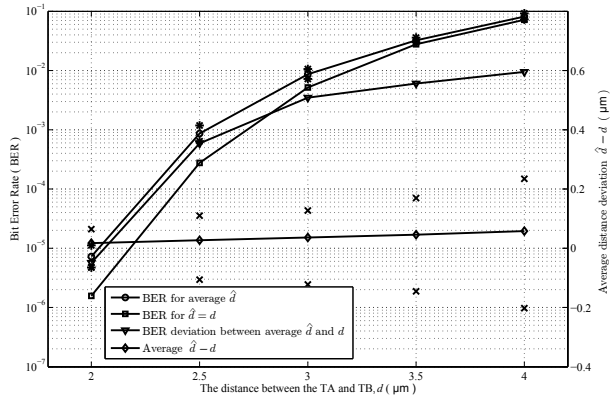

Figure 8: BER and the estimation deviation ($\hat{d}$-d) Vs. d with $T_e = 1000\,\mu\text{s}$ and $I = 20$. The dashed line between two '$*$' or '$\times$' symbols represents the variation range of the BER or deviation.

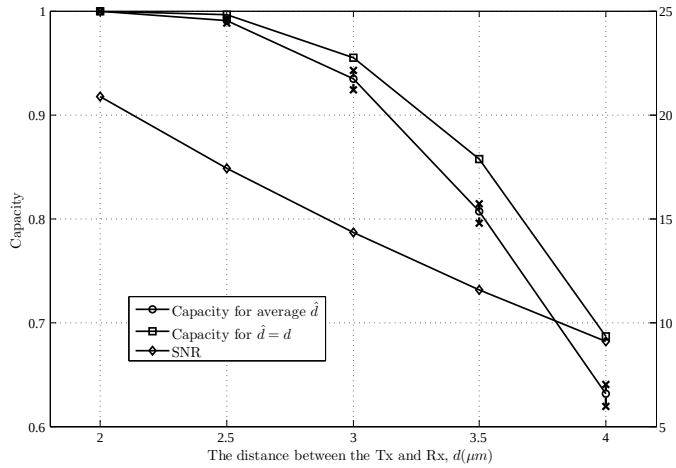

Figure 9: SNR and capacity Vs. d with $T_e = 1000\,\mu\text{s}$ and $I = 20$. The dashed line between two '$\times$' symbols represents the variation range of the Capacity.

4.4. Channel performance analysis with the distance unknown

The performance evaluation with the distance estimation scheme implemented is presented in Figs. 8 and 9. As is clearly shown, with the distance d getting larger, the system tends to suffer from a higher BER and correspondingly lower capacity. When d increases, it can be deduced from (3) that fewer molecules will arrive at the NB. In this case, any slight change of the concentration will significantly affect the decoding process of the NB, which can be also explained as the system has a smaller SNR according to (3) through (11). Thus, the system will have a weak resistance against the influence of the noise and ISI.

Another important feature is that, with d rising, the distance estimation accuracy goes down, leading to a larger difference in the BER between the system with distance pre-known ($\hat{d} = d$) and the system with distance to measure. It can therefore be deduced that by improving the

estimation accuracy, there will be less error occurrence in the system. An obvious method to enhance the system performance is to increase the SNR of the system. With a larger SNR, not only can the estimation be more accurate, but also the system will suffer less from the impact of the channel noise and memory. It can be deduced from Section 4.2 that three options can be applied to increase the SNR, i.e., increasing m, decreasing T_e, and further mitigating the influence of the ISI.

5. Conclusions

In this paper, a new decoding algorithm with an optimised threshold is proposed for a concentration-based MC system, which has been refined by taking the TN emission process into consideration. Based on this model, an information theoretical approach has been proposed to evaluate the system performance in terms of the BER and channel capacity. Simulations have also been carried out to verify the accuracy of these analytical formulations, and the cause of the deviation between the theoretically derived and simulated results has been explained. Numerical results illuminate that the BER and capacity are highly dependent on the number of molecules emitted per pulse (m), the emission duration (T_e), the ISI length (I) and the distance between the NA and NB (d). System performance for OT and MSE decoding techniques is compared to show the superiority of this new decoding algorithm. Moreover, this is the first investigation on the performance of MC systems with the distance unknown for nano-machines. Comparisons between distance-preknown systems and distance-unknown systems have been made, and results reveal that the performance can be enhanced by three methods, releasing more molecules, releasing molecules faster, and mitigating the influence of the ISI and the noise.

References

[1] Atakan B, Akan OB. An information theoretical approach for molecular communication. In: International Conference on Bio-Inspired Models Networks, Information, and Computing Systems. 2007, p. 33–40. doi:10.1109/BIMNICS.2007.4610077.

[2] Pierobon M, Akyildiz IF. Capacity of a diffusion-based molecular communication system with channel memory and molecular noise. IEEE Transactions on Information Theory 2013;59(2):942–954. doi:10.1109/TIT.2012.2219496.

[3] Eckford AW. Achievable information rates for molecular communication with distinct molecules. In: International Conference on Bio-Inspired Models Networks, Information, and Computing Systems. 2007, p. 313–315. doi: 10.1109/BIMNICS.2007.4610135.

[4] Mosayebi R, Arjmandi H, Gohari A, Nasiri-Kenari M, Mitra U. Receivers for diffusion-based molecular communication: Exploiting memory and sampling rate. IEEE Journal on Selected Areas in Communications 2014;32(12):2368–2380. doi: 10.1109/JSAC.2014.2367732.

[5] Kim NR, Chae CB. Novel modulation techniques using isomers as messenger molecules for nano communication networks via diffusion. IEEE Journal on Selected Areas in Communications 2013;31(12):847–856. doi:10.1109/JSAC.2013.SUP2.12130017.

[6] Kilinc D, Akan OB. Receiver design for molecular communication. IEEE Journal on Selected Areas in Communications 2013;31(12):705–714. doi:10.1109/JSAC.2013.SUP2.1213003.

[7] ShahMohammadian H, Messier GG, Magierowski S. Optimum receiver for molecule shift keying modulation in diffusion-based molecular communication channels. Nano Communication Networks 2012;3(3):183 –195. doi: http://dx.doi.org/10.1016/j.nancom.2012.09.006.

[8] Llatser I, Cabellos-Aparicio A, Pierobon M, Alarcon E. Detection techniques for diffusion-based molecular communication. IEEE Journal on Selected Areas in Communications 2013;31(12):726–734. doi:10.1109/JSAC.2013.SUP2.1213005.

[9] Atakan B, Akan OB. On channel capacity and error compensation in molecular communication. In: Transactions. on Computational Systems Biology X; vol. 5410 of *Lecture Notes in Computer Science*. Springer Berlin Heidelberg; 2008, p. 59–80. doi:10.1007/978-3-540-92273-5-4.

[10] Kuran MS, Yilmaz HB, Tugcu T, Akyildiz IF. Modulation techniques for communication via diffusion in nanonetworks. In: IEEE International Conference on Communications (ICC). 2011, p. 1–5. doi:10.1109/icc.2011.5962989.

[11] Nakano T, Okaie Y, Liu JQ. Channel model and capacity analysis of molecular communication with brownian motion. IEEE Communications Letters 2012;16(6):797–800. doi: 10.1109/LCOMM.2012.042312.120359.

[12] Moore MJ, Suda T, Oiwa K. Molecular communication: Modeling noise effects on information rate. IEEE Transactions on NanoBioscience 2009;8(2):169–180. doi: 10.1109/TNB.2009.2025039.

[13] Singhal A, Mallik RK, Lall B. Molecular communication with brownian motion and a positive drift: performance analysis of amplitude modulation schemes. IET Communications 2014;8(14):2413–2422. doi:10.1049/iet-com.2013.0939.

[14] Chahibi Y, Akyildiz IF. Molecular communication noise and capacity analysis for particulate drug delivery systems. IEEE Transactions on Communications 2014;62(11):3891–3903. doi: 10.1109/TCOMM.2014.2360678.

[15] Singhal A, Mallik RK, Lall B. Effect of molecular noise in diffusion-based molecular communication. IEEE Wireless Communications Letters 2014;3(5):489–492. doi: 10.1109/LWC.2014.2345756.

[16] Mahfuz MU, Makrakis D, Mouftah HT. On the characterization of binary concentration-encoded molecular communication in nanonetworks. Nano Communication Networks 2010;1(4):289 – 300. doi:http://dx.doi.org/10.1016/j.nancom.2011.01.001.

[17] Yilmaz HB, Chae CB. Simulation study of molecular communication systems with an absorbing receiver: Modulation and ISI mitigation techniques. Simulation Modelling Practice and Theory 2014;49:136 – 150. doi: http://dx.doi.org/10.1016/j.simpat.2014.09.002.

[18] Wang X, Higgins MD, Leeson MS. Distance estimation schemes for diffusion based molecular communication systems. IEEE Communications Letters 2015;19(3):399–402. doi: 10.1109/LCOMM.2014.2387826.

[19] Wang X, Higgins MD, Leeson MS. Relay analysis in molecular communications with time-dependent concentration. IEEE Communications Letters 2015;19(11):1977–1980. doi: 10.1109/LCOMM.2015.2478780.

[20] Moore MJ, Nakano T, Enomoto A, Suda T. Measuring distance from single spike feedback signals in molecular communication. IEEE Transactions on Signal Processing 2012;60(7):3576–3587. doi:10.1109/TSP.2012.2193571.

[21] Huang JT, Lai HY, Lee YC, Lee CH, Yeh PC. Distance estimation in concentration-based molecular communications. In: IEEE Global Communications Conference (GLOBECOM). 2013, p. 2587–2591. doi:10.1109/GLOCOM.2013.6831464.

[22] Ahmadzadeh A, Noel A, Schober R. Analysis and design of multi-hop diffusion-based molecular communication networks. IEEE Transactions on Molecular , Biological and Multi-Scale Communications 2015;(1)(6):144–157. doi: 10.1109/TMBMC.2015.2501741.

[23] Pierobon M, Akyildiz IF. Diffusion-based noise analysis for molecular communication in nanonetworks. IEEE Transactions on Signal Processing 2011;59(6):2532–2547. doi: 10.1109/TSP.2011.2114656.
[24] Aminian G, Arjmandi H, Gohari A, Kenari MN, Mitra U. Capacity of LTI-Poisson channel for diffusion based molecular communication. In: IEEE International Conference on Communications (ICC). 2015 p. 1060–1065. doi:10.1109/ICC.2015.7248463.
[25] Rodriguez-Henriquez F, Rocha-Perez JM, Silva-Martineze J. Performance of a decision feedback demodulator in a time-dispersive channel for ISI cancellation and its implementation in switched-capacitor technique. In: IEEE International Symposium on Personal, Indoor and Mobile Radio Communications (PIMRC). 1999, p. 1–5.

Xiayang Wang received the degree of Bachelor of Science majoring in Opto-information Science and Technology from the Department of Optoelectronics Science and Technology in Huazhong University of Science and Technology, China, in 2011. In 2013, he graduated from the Department of Electronics at the University of York, receiving a First Class Honors MSc degree in Communications Engineering. Xiayang then moved to the University of Warwick where he is currently working towards his PhD in Nano-communications.

Yi Lu received the degree of Bachelor of Engineering with First Class Honors in Electronic Engineering from University of Central Lancashire, UK, in 2011. And then she obtained a Master degree of Engineering with Distinction in Electronic Engineering from University of Sheffield, UK, in 2012. She is currently a scholarship student pursuing a PhD study in Nano-communications at University of Warwick.

Matthew D. Higgins Matthew Higgins received his MEng in Electronic and Communications Engineering and his PhD in Engineering from the School of Engineering at the University of Warwick in 2005 and 2009 respectively. Remaining at the University of Warwick, he then progressed through several Research Fellow positions, in association with some of the UKs leading defence and telecommunications companies before undertaking two years as a Senior Teaching Fellow in Telecommunications, Electrical Engineering and Computer Science subjects. In July 2012, Dr Higgins was promoted to the position of Assistant Professor where his research focused on Optical, Nano, and Molecular Communications. Whilst is this position, Dr Higgins set up the Vehicular Communications Research Laboratory which aimed to enhance the use of communications systems within the vehicular Space. As of March 2016, Dr Higgins was appointed as an Associate Professor at WMG working in the area of Connected and Autonomous Vehicles. Dr Higgins is a Senior Member of the IEEE, SMIEE, a member of the IEEE Communications Society, COMSOC, and a Fellow of the Higher Education Academy, FHEA.

Mark S. Leeson received the degrees of BSc and BEng with First Class Honors in Electrical and Electronic Engineering from the University of Nottingham, UK, in 1986. He then obtained a PhD in Engineering from the University of Cambridge, UK, in 1990. From 1990 to 1992 he worked as a Network Analyst for National Westminster Bank in London. After holding academic posts in London and Manchester, in 2000 he joined the School of Engineering at Warwick, where he is now a Reader. His major research interests are coding and modulation, nanoscale communications and evolutionary optimisation. To date, Dr. Leeson has over 230 publications and has supervised fifteen successful research students. He is a Senior Member of the IEEE, a Chartered Member of the UK Institute of Physics and a Fellow of the UK Higher Education Academy.